

## Research Paper

# Platinum-Based Nanovectors Engineered with Immuno-Modulating Adjuvant for Inhibiting Tumor growth and Promoting Immunity

Lisha Liu<sup>1,2</sup>, Qinjun Chen<sup>1</sup>, Chunhui Ruan<sup>1</sup>, Xinli Chen<sup>1</sup>, Yu Zhang<sup>1</sup>, Xi He<sup>1</sup>, Yujie Zhang<sup>1</sup>, Yifei Lu<sup>1</sup>, Qin Guo<sup>1</sup>, Tao Sun<sup>1</sup>, Hao Wang<sup>2</sup>, Chen Jiang<sup>1</sup>✉

1. Key Laboratory of Smart Drug Delivery, Ministry of Education, State Key Laboratory of Medical Neurobiology, Department of Pharmaceutics, School of Pharmacy, Fudan University, Shanghai 200032, China
2. China National Pharmaceutical Engineering and Research Center, China State Institute of Pharmaceutical Industry, Shanghai 201203, China

✉ Corresponding author: Chen Jiang, Key Laboratory of Smart Drug Delivery, Ministry of Education, State Key Laboratory of Medical Neurobiology, Department of Pharmaceutics, School of Pharmacy, Fudan University, Shanghai 200032, China; E-mail: jiangchen@shmu.edu.cn

© Ivyspring International Publisher. This is an open access article distributed under the terms of the Creative Commons Attribution (CC BY-NC) license (<https://creativecommons.org/licenses/by-nc/4.0/>). See <http://ivyspring.com/terms> for full terms and conditions.

Received: 2017.11.30; Accepted: 2018.02.16; Published: 2018.04.18

## Abstract

Although there is ample evidence that the chemotherapeutic drugs trigger an immune response, the efficient tumor rejection or regression is not guaranteed probably due to the massive immunosuppression within the tumor microenvironment. Thus, a rational delivery platform that overcomes immunosuppression is needed to maximally achieve both cytotoxic and immune-modulatory functions of chemotherapeutics. Accumulating evidence suggests that platinum-based drugs might be suitable for this application.

**Methods:** The dendrigraft polylysine (DGL) with its uniform size and multifunctional groups was employed as the polymeric core and conjugated with platinum-based compounds as therapeutics and WKYMMV peptide (Wpеп) as a targeting ligand to construct the novel delivery platform Wpеп-DGL/Pt. A series of *in vitro* and *in vivo* analyses, including physical and chemical characterizations, targeting property, biosafety, and antitumor efficacy of Wpеп-DGL/Pt were systematically carried out.

**Results:** Wpеп-DGL/Pt showed potent antitumor efficacy in MDA-MB-231 cells tumor-bearing nude mice with a deficient immune system, demonstrating targeted delivery of chemotherapeutics and the resultant cytotoxicity. Furthermore, in immunocompetent mice bearing 4T1 cells tumors, Wpеп-DGL/Pt activated immune cells and induced cell death proving their dual function of chemotherapeutic and immunomodulatory efficacy.

**Conclusion:** This work represents a novel approach for cancer immunotherapy by integrating nanotechnology and platinum-based therapeutics which not only efficiently exerts the chemotherapeutic cytotoxic effect on tumor cell but also restores immune response of immunological cells within the tumor microenvironment.

Key words: tumor immune microenvironment, platinum, chemotherapy, immune response

## Introduction

During the past decades, the paradigm for cancer treatment has shifted from nonspecific chemotherapeutics to more specific protective immunotherapy. With a better understanding of molecular details in tumor immunology and tumor

biology, tailored cancer immunotherapy is considered as a promising strategy for cancer treatment. For example, antibodies specific to tumor antigens, adoptively transferred immune cells, therapeutic vaccines, and recombinant cytokines effectively boost

the host immune system to recognize tumor cells as pathogens and eliminate them [1-3]. Cancer immunotherapy approaches designed to surmount tumor suppression take into consideration the pivotal molecular processes involved in the activation of immune system. First, the stimulatory or death signals are released from apoptotic tumor cells into the tumor microenvironment. Then these signals are engulfed as antigens and presented by antigen-presenting cells within the tumor-derived lymph nodes. Finally, the innate immunity or adaptive immunity is stimulated leading to regulation and inhibition of tumor growth.

During the early phase of tumor development, immune cells could spontaneously infiltrate into the tumor microenvironment to evoke an immune response and fight against the growth of the tumor. However, this protective mechanism eventually fails. Several mechanisms have been identified that may help tumor cells avoid recognition and destruction by the immune system, including down-regulation of major histocompatibility complex (MHC) class I expression on their surface to escape recognition by cytotoxic T cells, resistance to cytotoxic T lymphocyte-mediated apoptosis, and inhibition by immunosuppressive molecules within tumor microenvironment [4]. Thus, the tumor microenvironment is characterized by massive immunosuppression, and, therefore, the efficient restoration of infiltrating immune cells' function is becoming a promising approach for cancer immunotherapy.

Due to the intricate tumor microenvironment, the success of immunotherapy depends primarily on the regulation of immune effector cells infiltrated into the tumor tissues [5]. Hence, both cancer immunology and tumor microenvironment should be taken into consideration and combined for developing more precise therapeutics. Recently, preclinical reports have suggested that some conventional chemotherapeutics could stimulate the activation of the innate and/or adaptive immune cells in the tumor microenvironment [6-8]. Specifically, some cytotoxic agents are capable of inducing the immunogenic cell death (ICD) of tumor cells and send the "eat-me" signal to antigen presenting cells (e.g., dendritic cells, macrophages), resulting in monocyte/NK cells-dependent antitumor immunity and sensitizing tumor cells to cytotoxic T lymphocytes [9-13]. These immune-stimulatory characteristics make chemotherapeutic agents ideal adjuvants for cancer immunotherapy in addition to their cytotoxic effect on tumor cells. Thus, a rational approach exploiting the immune-chemotherapeutic function not only reduces the tumor size but also, more significantly, triggers the dormant innate immune response to eliminate any

residual cancer cells.

In our previous research, we utilized a peptide ligand, termed as the WKYMVm peptide, to modify nanoparticles for enhancing the drug accumulation in tumor loci. WKYMVm is the binding ligand for formyl peptide receptors (FPRs), which are selectively overexpressed in several malignant tumors, such as glioma, gastric cancer, and breast cancer [14-16]. FPRs ligands, like WKYMVm and fMLFK, are proven as potent immune adjuvants in activating innate immune cells, such as monocytes, dendritic cells, and NK cells, and have been utilized-as immune adjuvants to modulate the immune response [17, 18]. In the present study, WKYMVm was selected not only as a targeting molecule for tumor cells but also as an adjuvant peptide to assist chemo drugs in exerting the immune-stimulatory effect. We envisioned that a chemotherapeutic delivery platform modified by WKYMVm peptide could simultaneously exert direct cytotoxicity against malignant tumors and activate the immune response of tumor-infiltrated monocytes or NK cells.

Among various chemotherapeutic drugs, the platinum (Pt)-based therapeutics have shown clinical efficacy against many solid tumors [19]. Besides their principal mode of action in inhibiting DNA synthesis and repair, Pt drugs also engage in tumor-specific immune response by triggering the ICD effect on tumor cells, reversing the immunosuppressive tumor microenvironment, and stimulating innate immunity through improving monocyte- or natural killer cell-mediated cytotoxicity [20-22]. It has been reported that higher densities of tumor-infiltrating lymphocytes following Pt-based chemotherapy were correlated with significantly better survival outcomes [23]. Given this distinctive "off-target" immune modulatory effect of chemo drugs, a novel strategy of exploiting the immunogenic effect of Pt drugs would be promising in cancer immunotherapy. To achieve both cytotoxic and immune-stimulatory effects of Pt-based drugs, nanotechnology-based strategies have a great potential to improve drug delivery specifically to tumors and reduce severe side effects in normal tissues. Nanocarriers tend to accumulate in solid tumors due to the enhanced permeability and retention effect. Over the last few decades, researchers have developed various drug delivery systems such as liposomes, polymer nanoparticles, inorganic nanomaterials, and dendrimers [24-26]. Among them, dendrimers represent promising delivery vehicles due to their unique highly branched structure suitable to meet specific challenges. Our group has focused on dendrigraft polylysine (DGL) as a delivery system for small molecule drugs and/or gene drugs. Our results demonstrated that this multifunctional nanocarrier

could serve as an excellent delivery platform for cancers as well as brain diseases [27-29].

In this study, dichloro (1, 2-diaminocyclohexane) platinum (II) (DACHPt) was selected as the model drug, which has been demonstrated to show remarkable efficacy against several intractable tumors, such as triple-negative breast cancers, and has fewer side effects in patients [30]. We aimed to employ the Pt-based drug to trigger effective immune-modulatory chemotherapy. First, we constructed a DGL-based platform by conjugating DACHPt as the therapeutic agent and WKYMVm peptide (Wpep), a targeting ligand on cancer cells as well as an adjuvant for immune cells. The Wpep – DGL/Pt nano-therapeutic exhibited powerful efficacy on tumor cell apoptosis, which was evaluated in MDA-MB-231 cells and relevant animal models. The immune-modulatory chemotherapy stimulated monocytes- or NK cells-mediated cytotoxicity and induced ICD in 4T1 cells. Thus, the innovative treatment with the Wpep-DGL/Pt nano-therapeutic revealed promising antitumor outcome and immune-modulatory efficacy the outline of which is presented in the Schematic.

## Results and Discussion

### Synthesis and Characterization of Wpep-DGL/Pt Dendrimer

Pt-based drugs, which are used to treat almost 50% of cancer patients, suffer from severe systemic toxicity, poor tumor-targeted delivery, and considerable drug resistance. With the advancements in nanotechnology, Pt-based drugs have been incorporated into various nanocarriers, including liposomes, Au nanoparticles, and polymers, to prolong their circulation time and circumvent drug resistance [31-33]. Although DACHPt, the third generation of Pt-based drugs, is proven to be a broad-spectrum anticancer agent, it has poor solubility and inferior targeting ability. In this study, we selected diethylenetriaminepentaacetic acid (DTPA) as a chelating agent which was effectively integrated with DACHPt. This complex was further conjugated to DGL dendrimer with ample reactive surface groups. Subsequently, WKYMVm, a tumor-targeting ligand, was grafted on the surface of the DGL dendrimer through click chemistry using bifunctional polyethylene glycol (PEG) as the linker. A stepwise synthesis is illustrated in Figure 1A. DACHPt was treated with AgNO<sub>3</sub> to form the DACHPt intermediate, which was then chelated with *p*-SCN-Bn-DTPA to form DTPA-Pt. Next, DTPA-Pt was conjugated with PEG-DGL or Wpep-PEG-DGL to yield DGL/Pt or Wpep-DGL/Pt, respectively. Figure 1B shows <sup>1</sup>H-NMR spectra of

DGL/Pt in which H proton of lysine in the branching units of DGL displayed multiple peaks between 1.0 and 2.0 ppm. Peaks near 3.6 ppm exhibited the repeat units of PEG. The benzyl group in *p*-SCN-Bn-DTPA was around 7 ppm. The conjugation between Wpep and PEG-DGL was performed via click reaction with mild conditions and generated high yield. The spectrum of Wpep-DGL/Pt (Figure 1C), compared with that of DGL/Pt, appeared as a small peak near 7.8 ppm, representing the triazole group through the click chemistry between the alkyne group on W peptide and azide group on bifunctional PEG. The calculated Wpep: PEG: DGL: DTPA molar ratio was 5: 10: 1: 12. The <sup>1</sup>H-NMR result showed that one molecule of DTPA could chelate approximately five molecules of DACHPt resulting in the satisfactory drug loading efficiency. As our previous research has shown, DGLs is an excellent multifunctional drug delivery nanocarrier. Due to the presence of polyamine groups on DGLs, PEGylated DGL-Pts have high positive charges and enhanced stability [34, 35]. To achieve the dual-targeting purpose, W peptide, one of the FPR ligands overexpressed on tumor cells and innate immune cells, was successfully added on the DGL/Pt through the bifunctional PEG linker.

The average hydrodynamic diameter of Wpep-DGL/Pt was 18.25 nm measured by DLS which was consistent with the transmission electron microscopic (TEM) photograph (Figure 1D-E). Wpep-DGL/Pt exhibited spherical and monodisperse nanostructure enabling deep penetration in cancerous tissues.

### Anti-Proliferation Effect of the Dendrimer on MDA-MB-231 Cells

Oncogene expression contributes to the progressive proliferation of tumor cells. The platinum-based antineoplastic compounds inhibit proliferation of tumor cells by forming covalent Pt-DNA adducts. The cytotoxic effects of different Pt-based chemotherapeutics against FPRs-overexpressing MDA-MB-231 tumor cells were determined by the MTT assay after incubating the cells for 48 h. MDA-MB-231 cells were used to compare the cytotoxicity of Wpep-DGL/Pt with oxaliplatin and non-target modified DGL/Pt. As shown in Figure 2A, various Pt formulations could inhibit the cell viability in a dose-dependent manner with IC<sub>50</sub> values of 2728 ± 1.9, 1519 ± 1.3, and 611.4 ± 1.2 ng/mL for free oxaliplatin, DGL/Pt, and Wpep-DGL/Pt, respectively. Thus, the cytotoxic activity of Wpep-DGL/Pt was as potent as that of DGL/Pt, showing comparable IC<sub>50</sub> values. Furthermore, *in vitro* cytotoxicity of each dendrimer was higher than that of oxaliplatin, indicating that nanoparticles could improve the cellular uptake of the hydrophilic drug DACHPt.

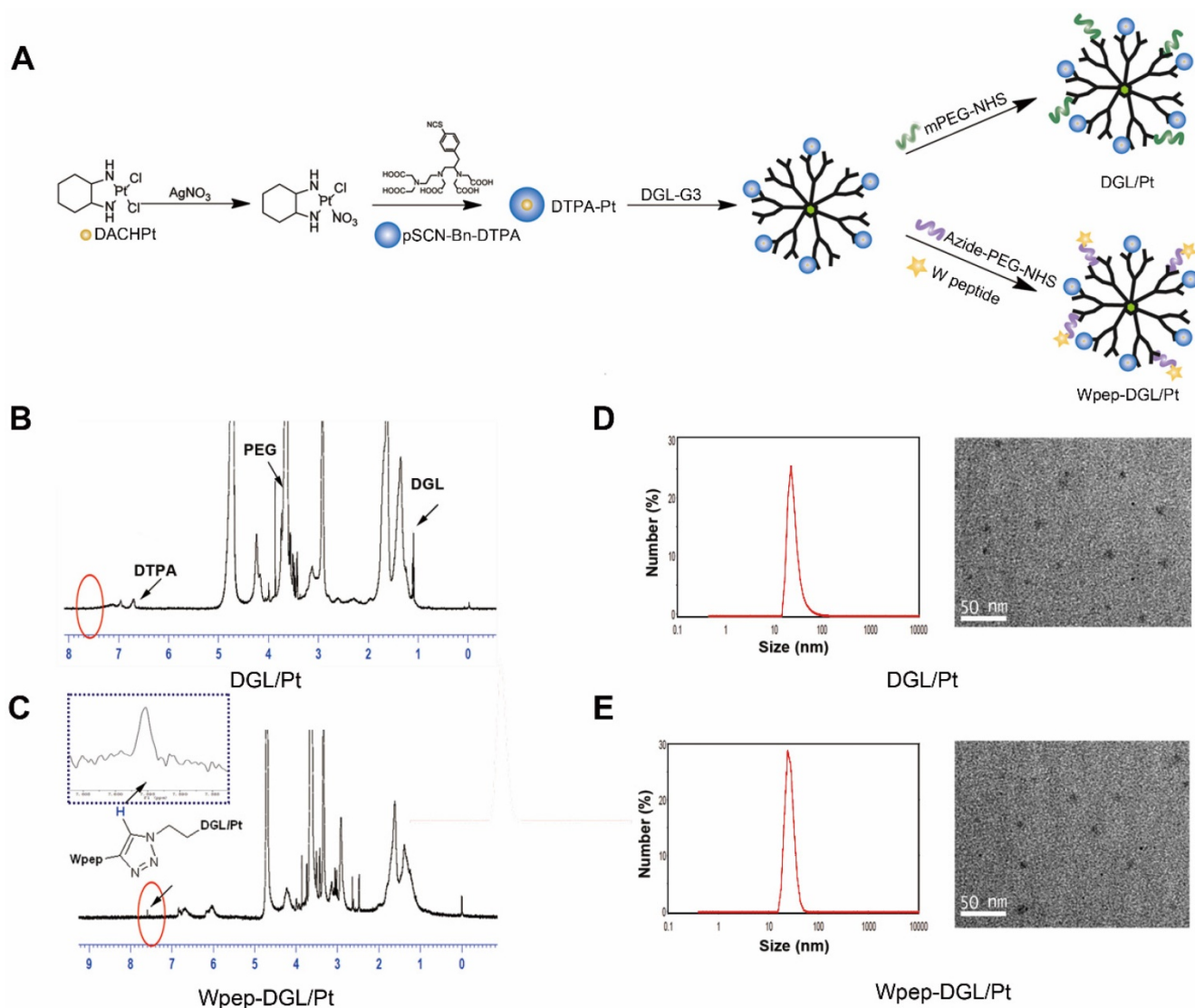


**Figure 1.** Synthesis route of DGL/Pt and Wpep-DGL/Pt (A);  $^1\text{H-NMR}$  spectrum of DGL/Pt in  $\text{D}_2\text{O}$  (B);  $^1\text{H-NMR}$  spectrum of Wpep-DGL/Pt (red circle indicates the triazole group) (C); morphological characterization of DGL/Pt and Wpep-DGL/Pt (D&E)

MDA-MB-231 cells overexpressing FPRs, bound the WKYMVm peptide and facilitated the higher cellular uptake of targeted Bodipy-Wpep-DGL/Pt than non-targeted Bodipy-DGL/Pt. The fluorescent intensity of each group is shown in Figure 2B. The internalization of Bodipy-Wpep-DGL/Pt by MDA-MB-231 cells was concentration-dependent. Consistent with the qualitative results, FACS data confirmed that the Bodipy signal of Wpep-DGL/Pt was higher than that of DGL/Pt. Also, the mean fluorescent intensities of Bodipy-Wpep-DGL/Pt exhibited a concentration-dependent tendency.

To understand the relative contribution of different endocytic pathways in Wpep-DGL/Pt-mediated internalization, MDA-MB-231 cells were pretreated with inhibitors against different endocytosis routes including PhAsO, colchicine, and filipin. As shown in Figure 2C, pre-incubation with W peptide significantly decreased the uptake of FPR ligand-

modified DGL/Pt. Among the three endocytosis inhibitors, filipin exhibited the strongest inhibitory effects, suggesting the internalization mechanism was mainly dependent on the caveolae-mediated pathway. Consistent with our previous work [36], quantitative results obtained from FACS analysis indicated that the mean fluorescent intensity in W peptide competition group was much lower than that in the other three endocytosis inhibitors-treated groups (Figure 2D). The Wpep-DGL/Pt displayed the most potent “killer” activity against tumor cells primarily attributable to the active targeting efficiency of W peptide and the pro-apoptotic role of platinum.

### Biodistribution and Anti-Tumor Efficacy of the Dendrimer in MDA-MB-231 Tumor-Bearing Mice

To demonstrate the targeting ability of Bodipy-Wpep-DGL/Pt and Bodipy-DGL/Pt, their

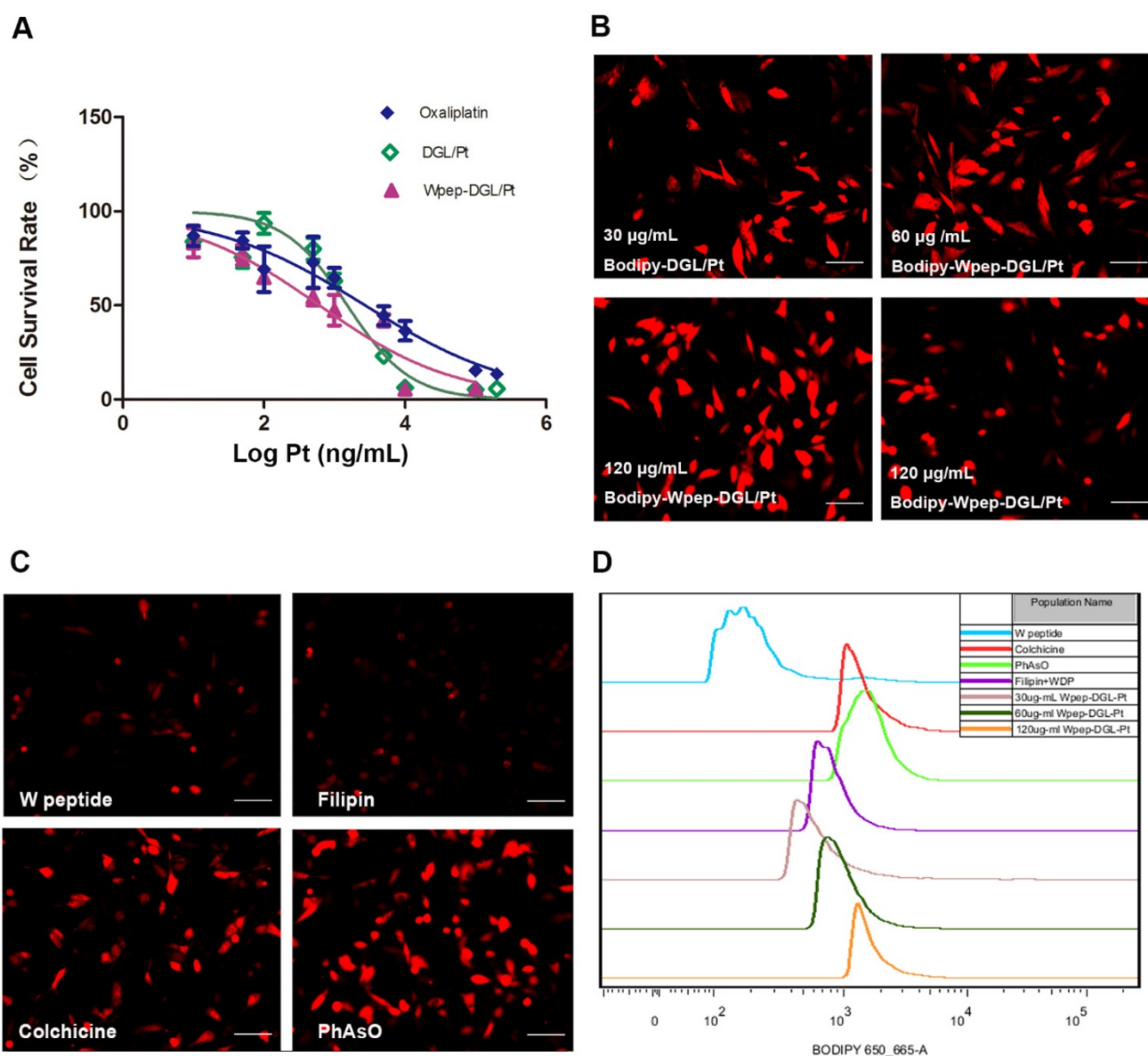


**Figure 2.** *In vitro* antiproliferative effect of Pt-based agents on MDA-MB-231 cells. (A) Cytotoxicity of Pt-based formulations at various concentrations against MDA-MB-231 cells after 48h incubation. Data are presented as mean±SD (n=6); (B) Cellular uptake of Bodipy-DGL/Pt and Bodipy-Wpep-DGL/Pt at different concentrations by the MDA-MB-231 cells after 30min incubation; (C) Possible uptake mechanism of Bodipy-Wpep-DGL/Pt internalization by the MDA-MB-231 cells. The cells were blocked by different inhibitors; (D) Flow cytometry analysis of cellular uptake and the uptake mechanism. Scale bar: 200 µm

biodistribution was examined in MDA-MB-231 tumor-bearing animal models. The targeting efficiency of the two groups was compared at different time points (Figure 3A). As time lapsed, the fluorescent signal of Bodipy-Wpep-DGL/Pt group was continuously accumulated in the tumor area due to the targeting function of Wpep. After 24 h post-injection, a 3D simulated image was constructed in Bodipy-Wpep-DGL/Pt group which confirmed the favorable targeting efficiency of W peptide in the tumor microenvironment. After the systemic administration, tumor and other major organs were harvested to evaluate the tissue distribution and tumor retention. A remarkably higher accumulation was observed in the tumors of Bodipy-Wpep-DGL/Pt

than that in Bodipy-DGL/Pt, suggesting that W peptide modification could decrease nonspecific distribution of DACHPt among the healthy tissues.

Therapy studies were conducted in the MDA-MB-231 tumor-bearing mice. For negative control, animals were injected with saline without any treatment. As depicted in Figure 4, compared with the oxaliplatin group, there was no change in animal body weight in the groups treated with Wpep-DGL/Pt or DGL/Pt. The two DGL groups elicited efficient tumor efficacy, proven with the stable and slight increase of tumor volume. The antitumor effect could be measured by tumor apoptosis using the terminal deoxynucleotidyl transferase dUTP nick-end labeling (TUNEL) assay. Both Wpep-DGL/Pt

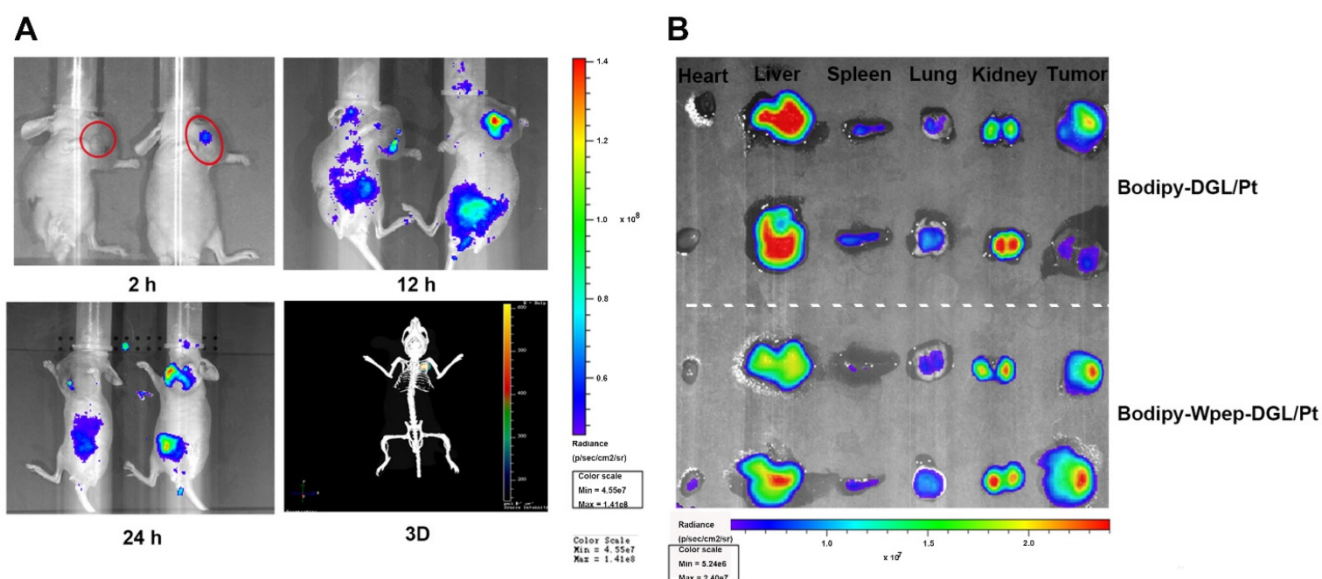


**Figure 3.** Biodistribution and targeting effects of Pt-based compounds in MDA-MB-231 tumor-bearing mice. (A) In vivo 2D imaging 2 h, 12 h and 24 h after i.v. injection of Bodipy-DGL/Pt (left) and Bodipy-Wpep-DGL/Pt(right) and 3D remodeling of Bodipy-Wpep-DGL/Pt captured after 24h of injection (red circle indicates the tumor area); (B) Representative ex vivo optical images of tumors and organs from MDA-MB-231 tumor-bearing mice sacrificed at 24h.

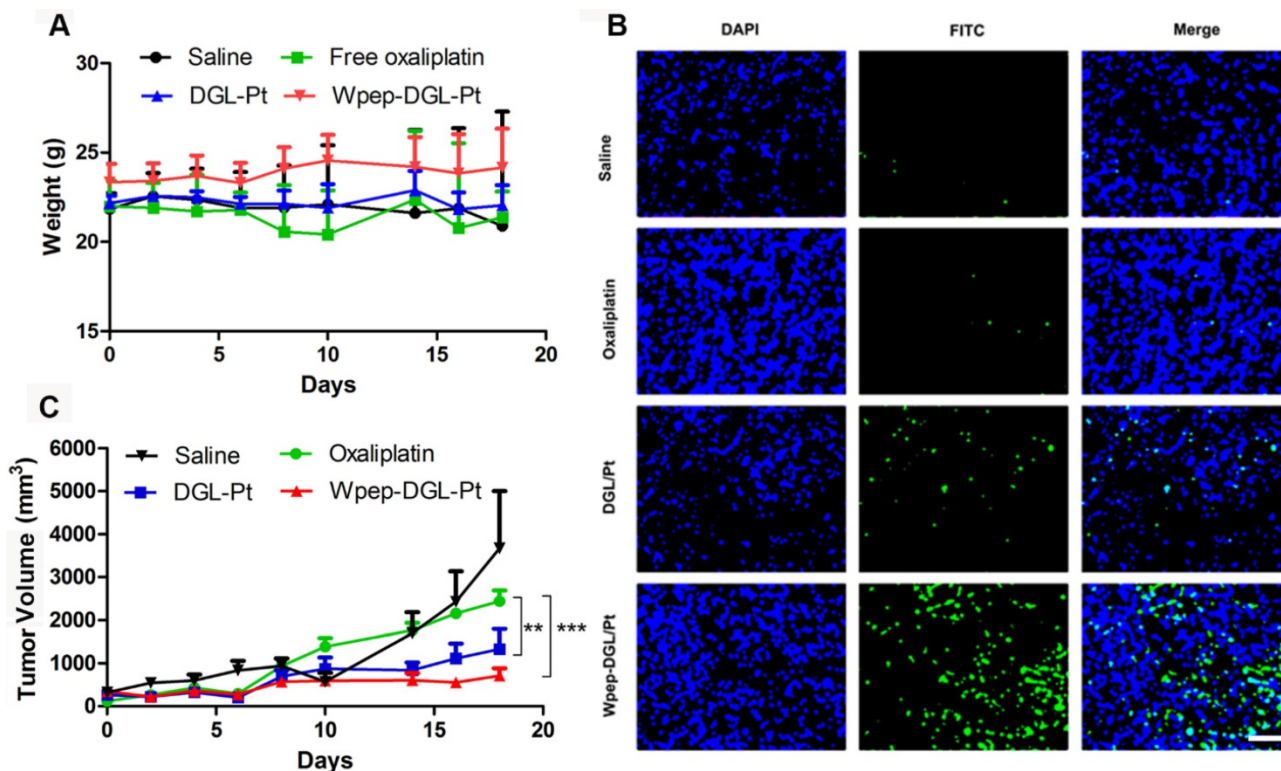


**Figure 4.** Antitumor efficacy of various Pt-based formulations on MDA-MB-231 tumor-bearing mice, evaluated for body weight (A), tumor volume (B), and TUNEL assay (C). (n=6, \*\*:p < 0.01; \*\*\*: p < 0.001). Scale bar: 100 μm

Pt and DGL/Pt-treated groups exhibited a comparable pro-apoptotic ability compared with the oxaliplatin group. Due to the targeting efficiency of Wpep-DGL/Pt, it exhibited the most potent antitumor activity revealing that Wpep-DGL/Pt exerted prominent pro-apoptotic function on cancerous tissues.

### Biosafety Test

Enhanced therapeutic efficacy might reduce the drug dosage as well as dosing frequency, alleviating side effects. H&E staining results (Figure 5) found no pathological abnormalities in the major organs between groups treated with Wpep-DGL/Pt and DGL/Pt, indicating the biosafety of nanocarriers.

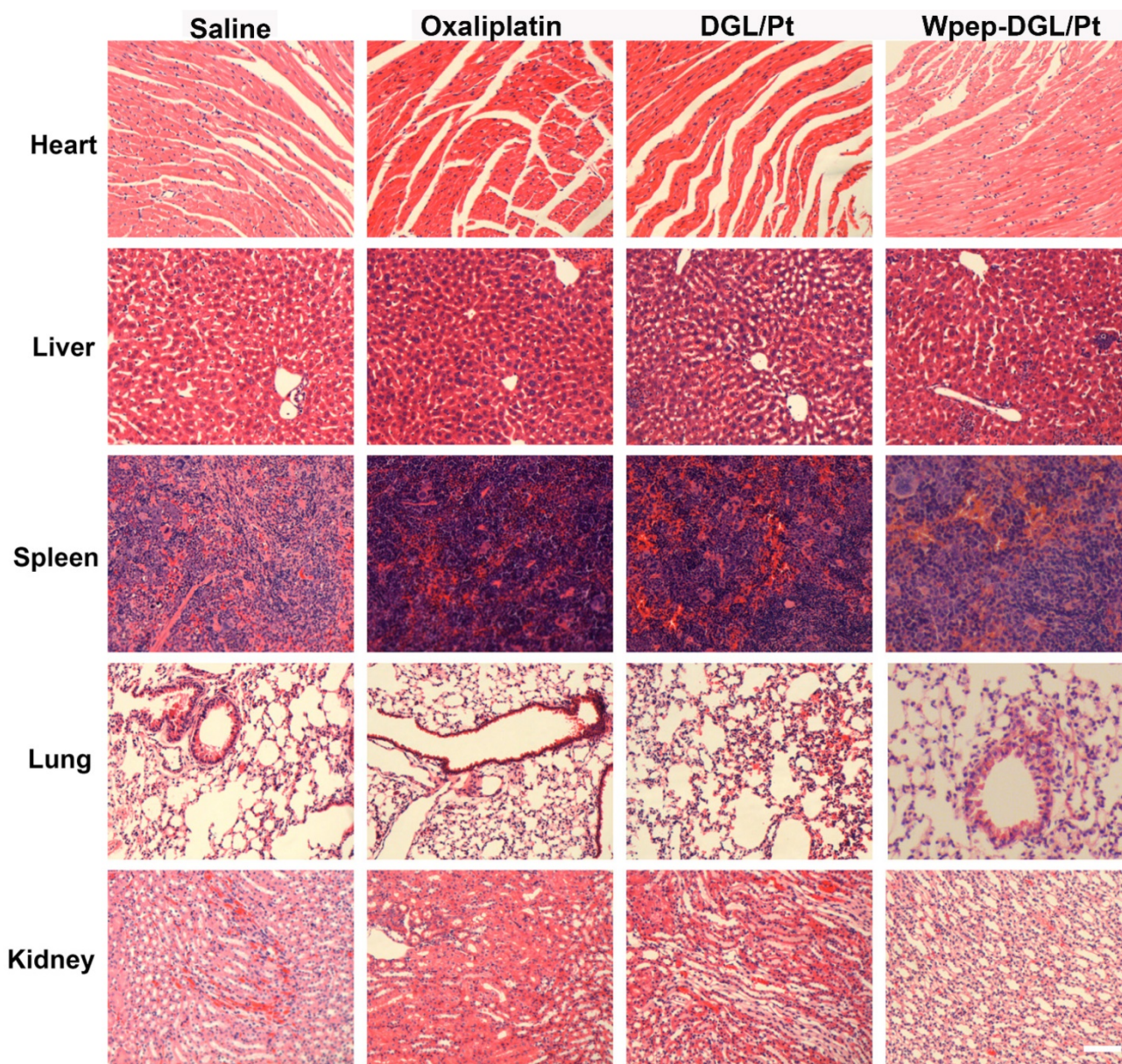


**Figure 5.** H&E staining for monitoring systemic toxicity of saline, oxaliplatin, DGL/Pt, and Wpep-DGL/Pt in MDA-MB-231 tumor-bearing mice. Scale bar: 100  $\mu$ m

### Cytotoxicity of Pt-Induced PBMCs against 4T1 Cells

Comparison between immunocompetent and immunodeficient mice suggested that certain chemotherapy drugs could induce tumor cell apoptosis and related immune response. The combination effect produced by Pt agent could be illustrated by two aspects. On the one hand, the pro-apoptotic effect could be induced by Pt agents on tumor cells as determined by the MTT assay. On the other hand, evidence exists that Pt-based chemo drugs could engage in the activation of native immune cells such as monocytes, NK cells, and macrophages and indirectly stimulate the immune system against malignant cells [21]. The validity of

immune-modulatory chemotherapy was further evaluated in animals with a viable immune system. It has been reported that immune cells could be evoked to engender immune cell-mediated cytotoxicity via various immune-regulatory strategies [37]. To demonstrate the tumoricidal effect of Pt-activated native immune cells, we first isolated murine peripheral blood mononuclear cells (mPBMCs), which expressed FPR receptors [38]. Next, an MTT-analogous experiment described by Daniel et al. was adopted to evaluate the immune cell-mediated cytotoxicity [39]. To investigate the immune-regulatory effect induced by Pt-based chemotherapeutics, mPBMCs were isolated, and the MTT-based test was used to evaluate the immune-cells-engendered cytotoxicity. The results

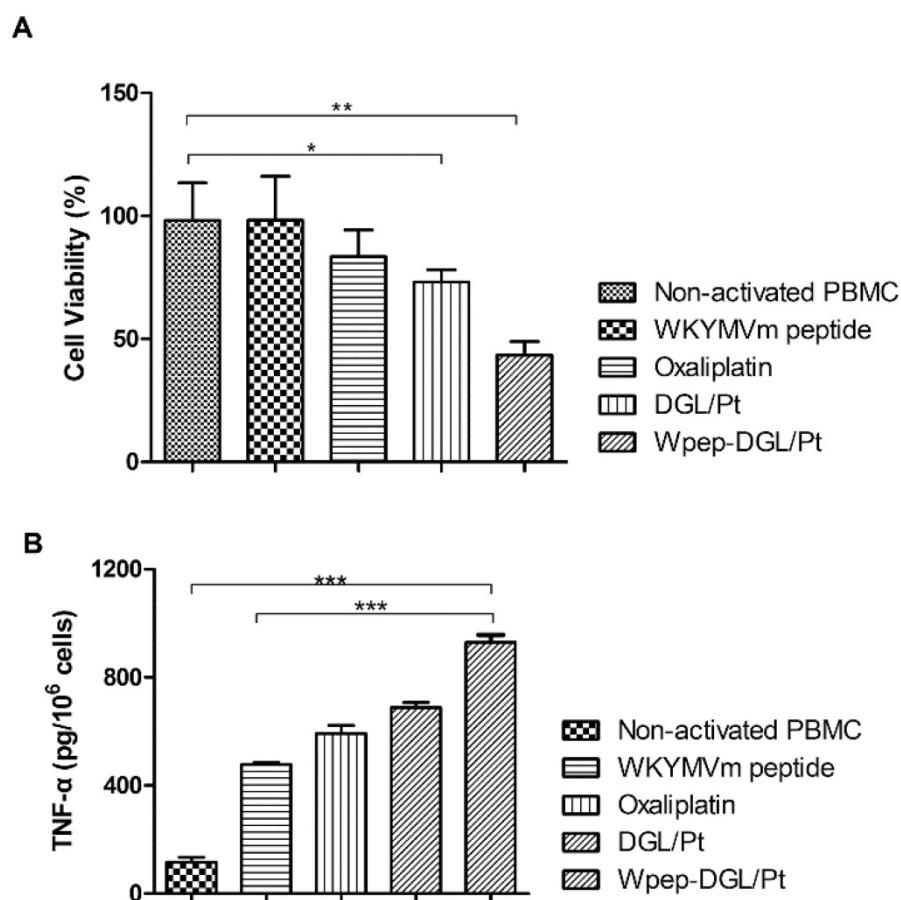


**Figure 6.** Pt-based formulations-induced immune cells-mediated cytotoxicity in 4T1 cells. (A) Cell viability measured as (%) of 4T1 cells when coincubated with treated mPBMCs after 72 h; (B) Secretion of proinflammatory cytokines (TNF- $\alpha$ ) by ELISA assay. (n=3, \*\*\*,  $p < 0.001$ ; \*\*,  $p < 0.01$ ; \*,  $p < 0.05$ )

indicated that the cell-mediated cytotoxicity against 4T1 cells of mPBMCs pretreated with Pt compounds for 24 h was significantly enhanced. As shown in Figure 6A, compared with DGL/Pt and oxaliplatin activated groups, Wpep-DGL/Pt was the most effective agent to boost the mPBMC-induced cytotoxicity. This suggested that increased intracellular Pt concentration contributed to enhanced activation of native immune cells and the adjuvant effect of the WKYMVm peptide on monocytes. In the absence of any activator in the culture media, non-activated mPBMCs exerted a pro-apoptotic effect on tumor cells. Also, although reported as an immune-stimulator, only W peptide-treated mPBMCs possessed significant immune cells-mediated cytotoxicity.

Because of its pivotal role in innate immunity [40], TNF- $\alpha$  was selected as the proinflammatory cytokine to measure the level of mPBMC activation. The extracellular level of the typical pro-inflammatory cytokine was determined to compare the level of immune cell activation induced by different groups (Figure 6). Immune cells could not be activated only by the Wpep as adjuvant in the absence of vaccine. All

groups treated with Pt-based activators exhibited a higher extracellular level of TNF- $\alpha$ . Especially, murine PBMCs treated with Wpep-DGL/Pt dramatically enhanced the secretion of TNF- $\alpha$ , which was higher than with DGL/Pt and oxaliplatin. Thus, the Pt-based regimen for cancer therapy was not only cytotoxic to tumor cells but also activated the dormant native immune cells in the tumor microenvironment.

### Immune-Modulatory Response and Anti-Tumor Efficacy of (the Dendrimer or) Wpep-DGL/Pt in 4T1 Tumor-Bearing Mice

In view of the immune-modulation capability of Wpep-DGL/Pt for mPBMCs *in vitro*, we explored the anti-tumor effect of Wpep-DGL/Pt *in vivo*. As illustrated by the data shown in Figure 7A-B, while free oxaliplatin injection showed no appreciable effect on both the tumor growth and the maintenance of body weight, Wpep-DGL/Pt significantly decreased the malignant growth of 4T1 tumors compared to other groups. The pro-apoptotic effect of Wpep-DGL/Pt, on the other hand, was comparable to other groups by the TUNEL assay (Figure 7C).

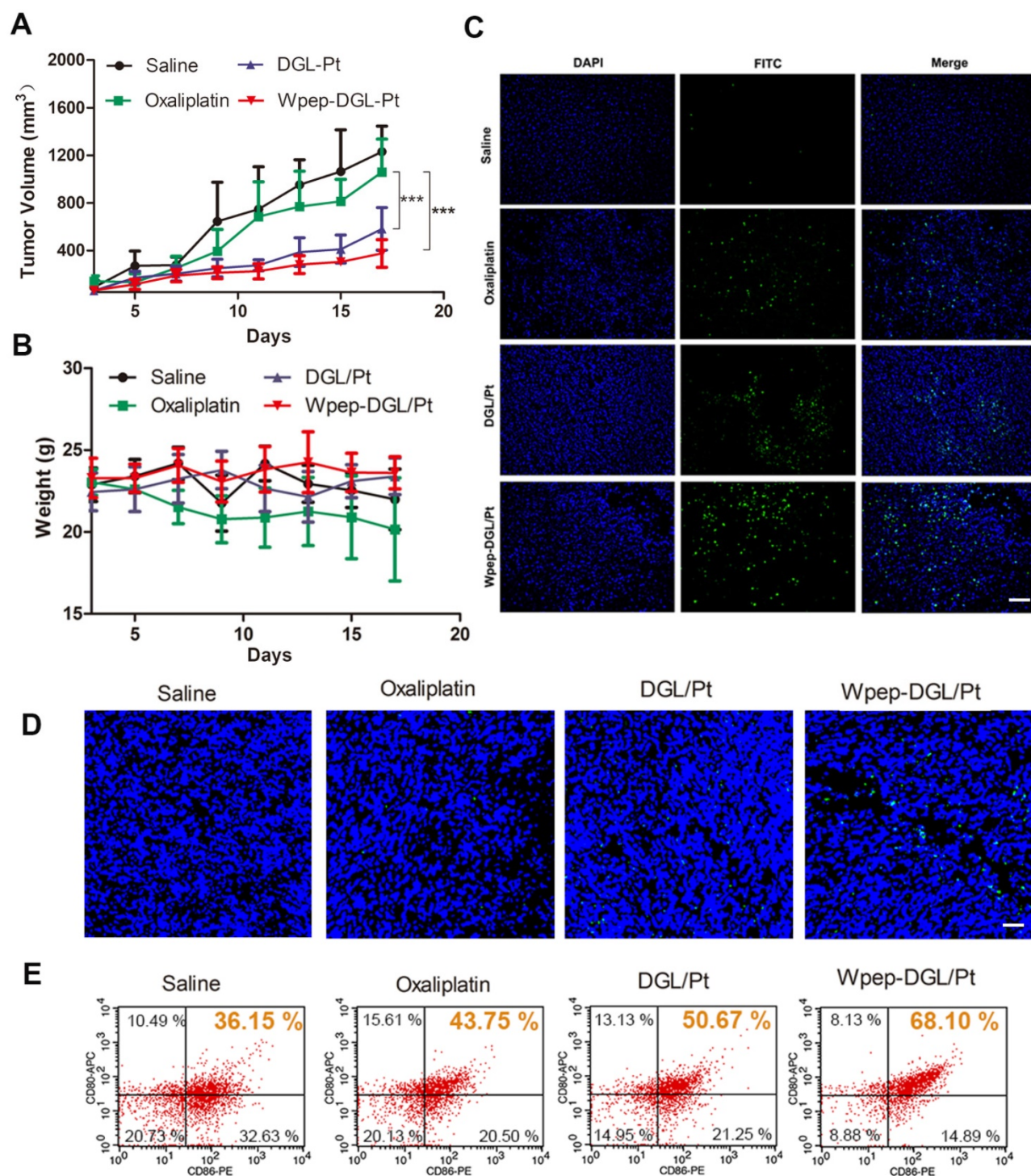


**Figure 7.** Immuno-modulating chemotherapeutic efficacy of various Pt-based formulations in 4T1 tumor-bearing mice evaluated as Tumor volume (A), body weight (B), TUNEL assay (C), CRT expression level (D) and DC maturation level (E). Scale bar: 100  $\mu$ m. (n=6, \*\*p < 0.01; \*\*\*: p < 0.001)

Although cytotoxic drugs inhibit the growth of rapidly proliferating tumor cells, there is increasing evidence to suggest that some of these drugs could aid immunotherapy by activating the immune system via specific mechanisms. For example, platinum drugs could not only induce immunogenic cell death but also promote dendritic cells maturation to counteract immune evasion [21]. Calreticulin (CRT)

exposure serves as a signal of immunogenic cell death. As shown in Figure 7D, the green fluorescence of CRT surrounded the blue fluorescence of the cell nucleus, which was consistent with the expression of CRT on the plasma membrane. After CRT exposure in the tumor microenvironment, these protein could be engulfed by DC or macrophages, considered as a powerful prerequisite for antigen presentation. DC

maturation level could be investigated to indirectly evaluate the immune-modulatory effect of different Pt agents. To compare the DC maturation level following various Pt-based treatments, mice were sacrificed to separate and measure the maturation level of DC resided in tumor-draining lymph nodes (TDLNs) by flow cytometry (Figure 7E). Pretreatment with Wpep-DGL/Pt could effectively induce CRT expression and resulted in a slight increase of DC maturation compared to other Pt-based therapies verifying the immune-modulatory effect of chemotherapy.

## Conclusion

We have reported the successful construction of a platinum-loaded DGL dendrimer tethered with an FPR-peptide, Wpep-DGL/Pt, as a delivery vehicle for dual-purpose targeting efficacy for tumor cells and immune cells. The results demonstrated that Wpep-DGL/Pt enhanced pro-apoptotic efficacy by efficient FPR-mediated endocytosis of tumor cells. In immune-deficient mice, significant accumulation at the tumor site was detected in the Wpep-DGL/Pt-treated group resulting in the most potent anti-tumor efficacy. The immune-regulatory properties of Wpep-DGL/Pt were also evaluated in immunocompetent models. The data indicated that platinum agents could induce activation of dormant immune cells indirectly enhancing the immune cells-mediated cytotoxicity to tumor cells. In the future, the exact mechanism between platinum-based drugs and immune system should be explored to have a better understanding of combined cytotoxic and immune-regulatory effects of chemotherapeutic drugs. This strategy of merging immune response and chemotherapy, as demonstrated by Wpep-DGL/Pt, was capable of enhancing apoptosis of cancer cells and inducing immune response.

## Materials and Methods

### Materials

DGL (containing 123 lysines, generation 3) was obtained from COLCOM (Montpellier Cedex, France). 2-(4-Isothiocyanatobenzyl)-diethylenetriaminepentaacetic acid (p-SCN-Bn-DTPA) was purchased from Macrocyclics (Dallas, TX, USA). DACHPt and oxaliplatin were purchased from Dalian Meilun Biotech Co., Ltd). Azide - polyethylene glycol -  $\omega$  - succinimidyl carbonate (Azide-PEG3500-NHS) was obtained from JenKem technology Co., Ltd. (Beijing, China). The WKYMVm peptide was synthesized by China Peptides Co., Ltd (Suzhou, China). Dulbecco's Modified Eagle's Medium (DMEM), Roswell Park Memorial Institute (RPMI) 1640 medium, and fetal

bovine serum (FBS) were purchased from Thermo Fisher Scientific Inc. (Waltham, USA). [4, 5-Dimethylthiazol-2-yl]-2, 5-diphenyl tetrazolium bromide (MTT) was purchased from Sigma-Aldrich (St. Louis, MO). BODIPY and DAPI were obtained from Thermo Fisher Scientific Inc. (Waltham, USA). One Step TUNEL Apoptosis Assay Kit was acquired from KeyGEN BioTECH (Nanjing, China). All other reagents were purchased from J & K Chemical Co., Ltd. (Shanghai, China).

### Synthesis of Wpep-DGL/Pt Dendrimer

DACHPt platinum drug was conjugated to DGL through DTPA as the linker. As described by Katoaka et al. [30], DACHPt was first suspended in distilled water and added to silver nitrate solution. The mixture was kept in the dark at room temperature overnight to form DACHPt nitrate chloride. After centrifugation and purification, DACHPt nitrate chloride was chelated with p-SCN-Bn-DTPA and reacted for 48 h to obtain Pt-DTPA. Subsequently, Pt-DTPA was purified by dialysis (MWCO: 3500 Da). Next, the amino group of DGL was conjugated with the isocyanate group of Pt-DTPA in pH 8.0 PBS for 48 h at room temperature to form DGL-Pt-DTPA. Unreacted Pt-DTPA was discarded by ultrafiltration (MWCO: 10000 Da), and DGL/Pt was linked with bifunctional Azide-PEG3500-NHS to obtain DGL/Pt dendrimer-based carrier and freeze-dried for storage. To tether W peptide to DGL/Pt, the alkyne group on W peptide was reacted with the azide group on bifunctional PEG from DGL/Pt/ via copper (I)-catalyzed azide-alkyne click chemistry. DGL/Pt and W peptide (2.5 equiv.) were mixed in DMF solution under nitrogen. A freshly prepared catalytic solution of CuI (0.5 equiv.), sodium ascorbate (2.5 equiv.), and DIPEA (2.5 equiv.) was added to the mixture, and the reaction was performed overnight at 35 °C. The final product, denoted as Wpep-DGL/Pt, was purified by dialysis against 10mM EDTA (pH 7.4 PBS) for 24 h, then against deionized water for 24 h. Finally, Wpep-DGL/Pt was lyophilized for storage.

### Characterization of Wpep-DGL/Pt Dendrimer

For structure characterization, DGL/Pt and Wpep-DGL/Pt were dissolved in D<sub>2</sub>O, and analyzed with a 400 MHz spectrometer (Varian, Palo Alto, CA, USA)

For morphologic properties, DGL/Pt and Wpep-DGL/Pt were observed by transmission electron microscopy (TEM, JEOL JEM-1200EX, Tokyo, Japan).

Drug loading efficiency (DL%) of Wpep-DGL/Pt and DGL/Pt were denoted as the platinum content, which was determined by inductively-coupled plasma - atomic emission spectroscopy (ICP-AES).

## Cell Culture

In the immune-deficient model, MDA-MB-231 cells were cultured in DMEM supplemented with 10% FBS and 1% v/v cocktail of antibiotic. While in the immune-competent model, 4T1 cells were cultured in RPMI 1640 supplemented with 10% FBS and 1% v/v cocktail of antibiotics. The cell lines were cultured in a 5% CO<sub>2</sub> incubator at 37 °C.

## Antitumor Efficacy of Wpеп-DGL/Pt Dendrimer on MDA-MB-231 Cells

The cytotoxicity of Platinum (Pt)-based delivery systems on MDA-MB-231 cells was evaluated by the MTT assay. MDA-MB-231 cells were seeded in 96-well plates at a density of  $5 \times 10^3$  cells/well and incubated for 24 h at 37 °C. Subsequently, spent media were discarded and replaced with fresh media containing free oxaliplatin or different Pt-based formulations ranging from various concentrations of Pt (0.018 ~ 682 µg/mL), and cells were cultured for 48 h. Control group was set up to represent cells without any treatment. Next, 100 µL MTT solution was added to each well and incubated for additional 4 h. The medium was then replaced with 150 µL DMSO per well and shaken for 10 min. The absorbance in each well was read at 570 nm using microplate spectrophotometer (Biotek).

The fluorescent dye BODIPY (excitation wavelength = 650 nm/emission wavelength = 665 nm) was conjugated on the surface of DGL/Pt or Wpеп-DGL/Pt in pH 8.0 PBS at room temperature for 2 h. Unreacted Bodipy was removed through dialysis (MWCO: 2000 Da). The MDA-MB-231 cells were seeded at a density of  $5 \times 10^4$  cells/well in 24-well plates and incubated at 37 °C for 24 h. When 80 ~ 90% confluence was achieved, the medium was replaced with 60 µg/mL Bodipy-DGL/Pt and Bodipy-Wpеп-DGL/Pt at a concentration of 30, 60 and 120 µg/mL for 0.5 h. Following the addition of 60 µg/mL of Bodipy-Wpеп-DGL/Pt, various inhibitors including 10 µM W peptide as receptor competitor and 0.5 µg/mL filipin, 1 µg/mL colchicine, 0.5 µg/mL phenylarane oxide (PhAsO) as endocytic inhibitors were preincubated with cells for 10 min. Subsequently, the incubated media were removed and washed three times with Hank's solution. For the qualitative analysis, cellular uptake of Pt formulations was visualized and photographed using a fluorescent microscope (Leica, Wetzlar, Germany). All images were captured with same imaging parameters to give a real comparison on the intensity of fluorescence of different formulations. For the quantitative analysis, cells were digested and resuspended in PBS, then analyzed by a flow cytometer (FACS Aria, BD, USA). Relative data were further processed with Flowjo 7.2.

The data were collected from a minimum of 10,000 events per sample.

## Antitumor Efficacy of Wpеп-DGL/Pt Dendrimer on MDA-MB-231 Tumor-Bearing Mice

All animal experiments were strictly complied with the guideline of Institutional Animal Care and Use Committee of China. Female Balb/c nude mice of ~20 g body weight were purchased from Department of Experimental Animals (Fudan University) and maintained under standard laboratory conditions. The xenograft tumor model was established by subcutaneous injection of  $1 \times 10^6$  MDA-MB-231 cells in 100 µL of 5 mg/mL Matrigel in PBS into the second right mammary fat pad of nude mice.

As mentioned above, BODIPY used in cell study could also be utilized in biodistribution experiments due to its near-infrared property. The non-targeted Bodipy-DGL/Pt and Bodipy-Wpеп-DGL/Pt were injected into the tail vein. Images were captured by IVIS Spectrum in vivo imaging system (Caliper, PerkinElmer, USA) at different time-points. After 24 h post-administration, the nude mice were anesthetized and sacrificed by injection of chloral hydrate via the tail vein. The principal organs were harvested for fluorescent imaging.

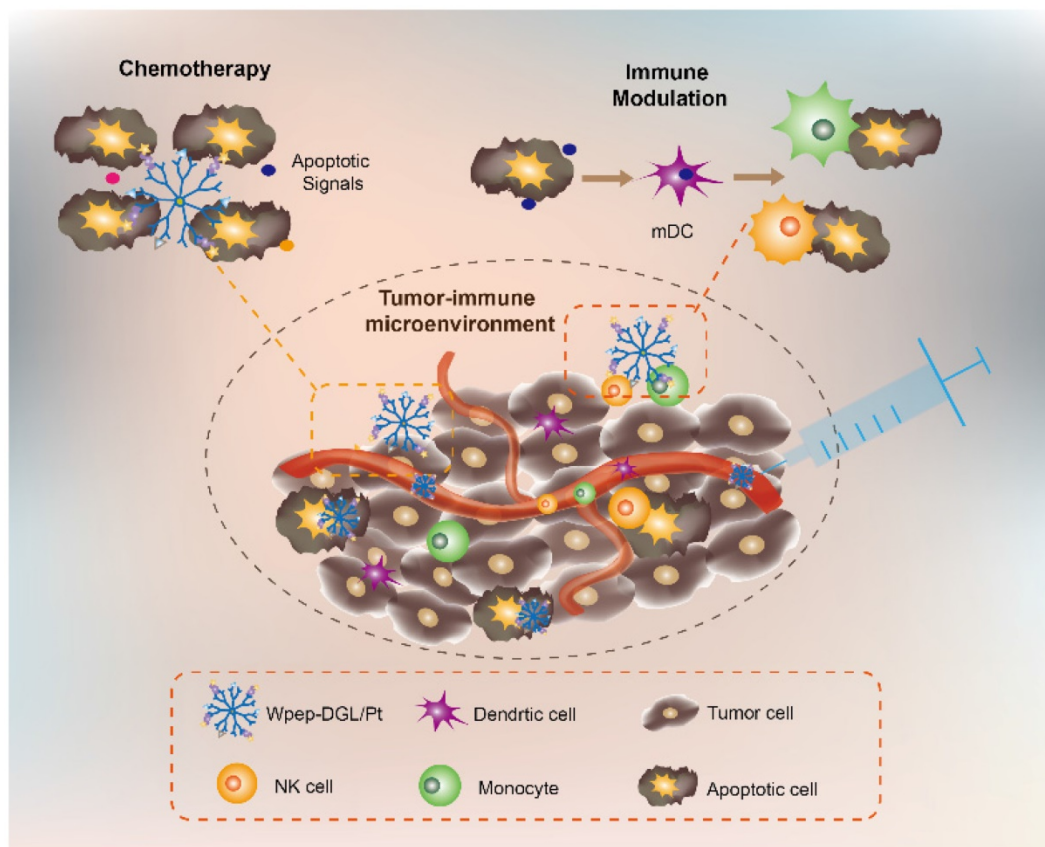
Antitumor efficacy was evaluated in MDA-MB-231 bearing Balb/c nude mice. Mice were randomly divided into four groups (n=6) and treated with oxaliplatin, DGL/Pt and Wpеп-DGL/Pt (an equal dose of 5 mg/kg), and saline (negative control). All the formulations were intravenously injected via tail vein for four times every 5 days. The body weight and tumor volume were measured every other day. The tumor volume was calculated according to the formula:  $h \times Width^2 \times 0.5$ . All mice were sacrificed on day 20.

TUNEL assay was performed on 5 µm frozen tumor slices using a DNA fragmentation detection kit according to the manufacturer's protocols and observed by fluorescent microscope. DNA fragments in apoptotic cells were stained with fluorescein - conjugated deoxynucleotide (green), and the nuclei were stained with DAPI.

For biosafety assay, mice were sacrificed after treatment with different Pt-based formulations. The principal organs were immediately fixed in 4% paraformaldehyde, embedded in paraffin, and sliced into 5mm- thick sections which were further stained with H & E for histological examination.

## Immuno-Modulatory Chemotherapy of Wpеп-DGL/Pt Dendrimer on 4T1 Cells

Peripheral blood mononuclear cells (PBMCs) were isolated from healthy Balb/c mice blood



**Scheme 1.** Illustration of both chemotherapy and immune-modulating effect of Wpеп-DGL/Pt.

(heparinized). The blood was mixed with pH 7.4 PBS (2:1, v:v) and layered over Ficoll/Paque (KeyGen BioTECH) and centrifuged according to the manufacturer's protocol. Mouse PBMCs were cultured in complete RPMI 1640 medium for 24 h at 37 °C.

For in vitro drug-induced immune cell-mediated cytotoxicity, a previously described procedure was followed [41]. PBMCs were activated by pretreating  $1 \times 10^5$  PBMCs with either 2  $\mu\text{M}$  of oxaliplatin, DGL/Pt, or Wpеп-DGL/Pt in a sterilized Eppendorf tube in 1 mL of complete RPMI medium for 24 h following gentle shaking at 37 °C. After activation, PBMCs were washed twice with and resuspended in 1 mL of complete RPMI medium. PBMCs were then co-cultured with the pre-seeded 4T1 cells (at a density of  $3 \times 10^3$  cells/well into 96-well plates) at a 10:1 ratio (effector cell: target cell). After incubation for 72 h, the medium was replaced by 100  $\mu\text{L}$ /well MTT solution for another 4 h incubation. Subsequently, MTT was discarded and substituted with 150  $\mu\text{L}$  DMSO per well. The absorbance in each well was read at 570 nm using microplate spectrophotometer (Biotek). Experiments were performed in triplicates.

The amount of the pro-inflammatory cytokines TNF- $\alpha$ , secreted by Pt-induced PBMCs after 24 h into the complete RPMI supernatant, was measured using

the commercially available mice TNF- $\alpha$  ELISA kit (QuantiCyto) according to the manufacturer's protocol. Calibration standards provided by the kits were reconstituted and diluted in complete RPMI. Readings were adjusted to pg/ $10^6$  cells for analysis.

### Immuno-Modulatory Chemotherapy of Wpеп-DGL/Pt Dendrimer on 4T1 Tumor-Bearing Mice

All animal experiments were strictly complied with the guideline of the Institutional Animal Care and Use Committee of Fudan University. Female Balb/c mice of ~20 g body weight were purchased from Department of Experimental Animals (Fudan University) and maintained under standard laboratory conditions. The xenograft tumor models were established as described previously. Upon reaching an approximate size of the tumor, oxaliplatin, DGL/Pt, Wpеп-DGL/Pt (at an equal dose of 5 mg/kg), or saline (negative control) was administered per mouse at a 10-day interval for 4 times. The body weight and tumor volume were measured every other day. All mice were sacrificed on day 20.

TUNEL assay was performed on 5  $\mu\text{m}$  frozen tumor slices using a DNA fragmentation detection kit according to the manufacturer's protocols and

observed by fluorescent microscope. DNA fragment in apoptotic cells was stained with fluorescein – conjugated deoxynucleotide (green), and the nucleus was stained with DAPI. The tumor tissues were stained with the anti-CRT antibody (Abcam) and observed under the confocal microscope. To analyze the DC maturation effect, tumor-draining lymph nodes were harvested after various Pt-based treatments. Cells were filtered through nylon mesh filters and washed with Hank's buffer. The single cell suspension was incubated with anti-CD86-PE (eBioscience), anti-CD80-APC (eBioscience) antibodies at 37 °C for 30 min and assessed using flow cytometry. Data analysis was carried out using FCS software.

### Statistical Analysis

Comparisons of parameters between two groups were performed with an unpaired Student t test, and comparisons of parameters among multiple groups were made with one-way analysis of variance. Data were presented as mean ± standard deviation (SD) unless otherwise indicated. A value of  $p < 0.05$  was considered statistically significant.

### Abbreviations

Bodipy: 6-({[4,4-Difluoro-5-(2-pyrrolyl)-4-bora-3a,4a-diaza-s-indacene-3-yl]styryloxy}acetyl)aminohe xanoic acid succinimidyl ester; CRT: calreticulin; DACHPT: dichloro (1, 2-diaminocyclohexane) platinum (II); DAPI: 4', 6-diamidino-2-phenylindole, dihydrochloride; DC: dendritic cell; DGL: dendrigraft polylysine; DTPA: diethylenetriaminepentaacetic acid; DL%: drug loading efficiency; DMEM: Dulbecco's modified eagle medium; DMSO: Dimethyl sulfoxide; FBS: fetal bovine serum; FACS: fluorescence-activated cell sorting; FPRs: formyl peptide receptors; H&E: hematoxylin-eosin staining; IC<sub>50</sub>: half maximal inhibitory concentration; ICD: immunogenic cell death; ICP-AES: inductively coupled plasma atomic emission spectrometry; MTT: 3-(4,5-dimethyl-2-thiazolyl)-2,5-diphenyl-2-H-tetrazolium bromide; MWCO: molecular weight cut off; PBMCs: peripheral blood mononuclear cells; PEG: polyethylene glycol; p-SCN-Bn-DTPA: 2-(4-Isothiocyanatobenzyl)-diethylenetriaminepentaacetic acid; RPMI 1640 Medium: Roswell park memorial institute 1640 medium; TDLNs: tumor-draining lymph nodes; TEM: transmission electron microscopy; TNF- $\alpha$ : tumor necrosis factor alpha; TUNEL: terminal deoxynucleotidyl transferase dUTP nick-end labeling; Wpеп: WKYMVm peptide; Wpеп-DGL-Pt: Wpеп modified DGL dendrimer conjugating with Pt-based drug.

### Acknowledgments

This work was supported by the grants from National Science Fund for Distinguished Young Scholars (grant no. 81425023) and the National Natural Science Foundation of China (grant no. 81373355).

### Competing Interests

The authors have declared that no competing interest exists.

### References

- Weiner LM, Surana R, Wang S. Monoclonal antibodies: versatile platforms for cancer immunotherapy. *Nat Rev Immunol*. 2010; 10: 317-327.
- Restifo NP, Dudley ME, Rosenberg SA. Adoptive immunotherapy for cancer: harnessing the T cell response. *Nat Rev Immunol*. 2012; 12: 269-281.
- Sharma P, Wagner K, Wolchok JD, Allison JP. Novel cancer immunotherapy agents with survival benefit: recent successes and next steps. *Nat Rev Cancer*. 2011; 11: 805-812.
- Gajewski TF, Schreiber H, Fu YX. Innate and adaptive immune cells in the tumor microenvironment. *Nat Immunol*. 2013; 14: 1014-1022.
- Ino Y, Yamazaki-Itoh R, Shimada K, Iwasaki M, Kosuge T, Kanai Y, et al. Immune cell infiltration as an indicator of the immune microenvironment of pancreatic cancer. *Br J Cancer*. 2013; 108: 914-923.
- Pfirschke C, Engblom C, Rickelt S, Cortez-Retamozo V, Garris C, Pucci F, et al. Immunogenic Chemotherapy Sensitizes Tumors to Checkpoint Blockade Therapy. *Immunity*. 2016; 44: 343-354.
- Liu WM, Fowler DW, Smith P, Dalgleish AG. Pre-treatment with chemotherapy can enhance the antigenicity and immunogenicity of tumours by promoting adaptive immune responses. *Br J Cancer*. 2010; 102: 115-123.
- Tang W, Yang J, Yuan Y, Zhao Z, Lian Z, Liang G. Paclitaxel nanoparticle awakens immune system to fight against cancer. *Nanoscale*. 2017; 9: 6529-6536.
- Gasser S, Raulat DH. The DNA damage response arouses the immune system. *Cancer Res*. 2006; 66: 3959-3962.
- Vacchelli E, Enot DP, Pietrocola F, Zitvogel L, Kroemer G. Impact of Pattern Recognition Receptors on the Prognosis of Breast Cancer Patients Undergoing Adjuvant Chemotherapy. *Cancer Res*. 2016; 76: 3122-3126.
- Dijkgraaf EM, Heusinkveld M, Tummers B, Vogelzoo LT, Goedemans R, Jha V, et al. Chemotherapy alters monocyte differentiation to favor generation of cancer-supporting M2 macrophages in the tumor microenvironment. *Cancer Res*. 2013; 73: 2480-2492.
- Kong M, Tang J, Qiao Q, Wu T, Qi Y, Tan S, et al. Biodegradable Hollow Mesoporous Silica Nanoparticles for Regulating Tumor Microenvironment and Enhancing Antitumor Efficiency. *Theranostics*. 2017; 7: 3276-3292.
- Li H, Li Y, Wang X, Hou Y, Hong X, Gong T, et al. Rational design of Polymeric Hybrid Micelles to Overcome Lymphatic and Intracellular Delivery Barriers in Cancer Immunotherapy. *Theranostics*. 2017; 7: 4383-4398.
- Khau T, Langenbach SY, Schuliga M, Harris T, Johnstone CN, Anderson RL, et al. Annexin-1 signals mitogen-stimulated breast tumor cell proliferation by activation of the formyl peptide receptors (FPRs) 1 and 2. *Faseb j*. 2011; 25: 483-496.
- Prevette N, Liotti F, Visciano C, Marone G, Melillo RM, de Paulis A. The formyl peptide receptor 1 exerts a tumor suppressor function in human gastric cancer by inhibiting angiogenesis. *Oncogene*. 2015; 34: 3826-3838.
- Cattaneo F, Guerra G, Ammendola R. Expression and signaling of formyl-peptide receptors in the brain. *Neurochem Res*. 2010; 35: 2018-2026.
- Kim SD, Lee HY, Shim JW, Kim HJ, Baek SH, Zabel BA, et al. A WKYMVm-containing combination elicits potent anti-tumor activity in heterotopic cancer animal model. *PLoS One*. 2012; 7: e30522.
- Wong DY, Yeo CH, Ang WH. Immuno-chemotherapeutic platinum(IV) prodrugs of cisplatin as multimodal anticancer agents. *Angew Chem Int Ed Engl*. 2014; 53: 6752-6756.
- Li Y, Deng Y, Tian X, Ke H, Guo M, Zhu A, et al. Multipronged Design of Light-Triggered Nanoparticles To Overcome Cisplatin Resistance for Efficient Ablation of Resistant Tumor. *ACS Nano*. 2015; 9: 9626-9637.
- Lesterhuis WJ, Punt CJ, Hato SV, Eleveld-Trancikova D, Jansen BJ, Nierkens S, et al. Platinum-based drugs disrupt STAT6-mediated suppression of immune responses against cancer in humans and mice. *J Clin Invest*. 2011; 121: 3100-3108.
- Hato SV, Khong A, de Vries IJ, Lesterhuis WJ. Molecular pathways: the immunogenic effects of platinum-based chemotherapeutics. *Clin Cancer Res*. 2014; 20: 2831-2837.
- Lu J, Liu X, Liao YP, Salazar F, Sun B. Nano-enabled pancreas cancer immunotherapy using immunogenic cell death and reversing immunosuppression. *Nat Commun*. 2017; 8: 1811.

23. Jochems C, Schlom J. Tumor-infiltrating immune cells and prognosis: the potential link between conventional cancer therapy and immunity. *Exp Biol Med* (Maywood). 2011; 236: 567-579.
24. He H, Lancina MG, 3rd, Wang J, Korzun WJ, Yang H, Ghosh S. Bolstering cholesteryl ester hydrolysis in liver: A hepatocyte-targeting gene delivery strategy for potential alleviation of atherosclerosis. *Biomaterials*. 2017; 130: 1-13.
25. Liu L, He H, Zhang M, Zhang S, Zhang W, Liu J. Hyaluronic acid-decorated reconstituted high density lipoprotein targeting atherosclerotic lesions. *Biomaterials*. 2014; 35: 8002-8014.
26. He H, Yuan Q, Bie J, Wallace RL, Yannie PJ, Wang J, et al. Development of mannose functionalized dendrimeric nanoparticles for targeted delivery to macrophages: use of this platform to modulate atherosclerosis. *Transl Res*. 2017.
27. Kuang Y, Jiang X, Zhang Y, Lu Y, Ma H, Guo Y, et al. Dual Functional Peptide-Driven Nanoparticles for Highly Efficient Glioma-Targeting and Drug Codelivery. *Mol Pharm*. 2016; 13: 1599-1607.
28. Liu Y, An S, Li J, Kuang Y, He X, Guo Y, et al. Brain-targeted co-delivery of therapeutic gene and peptide by multifunctional nanoparticles in Alzheimer's disease mice. *Biomaterials*. 2016; 80: 33-45.
29. Liu Y, He X, Kuang Y, An S, Wang C, Guo Y, et al. A bacteria deriving peptide modified dendrigraft poly-L-lysines (DGL) self-assembling nanoplatform for targeted gene delivery. *Mol Pharm*. 2014; 11: 3330-3341.
30. Cabral H, Murakami M, Hojo H, Terada Y, Kano MR, Chung UI, et al. Targeted therapy of spontaneous murine pancreatic tumors by polymeric micelles prolongs survival and prevents peritoneal metastasis. *Proc Natl Acad Sci U S A*. 2013; 110: 11397-11402.
31. Kumar D, Lee SB, Park CH, Kim CS. Impact of Ultrasmall Platinum Nanoparticle Coating on Different Morphologies of Gold Nanostructures for Multiple One-Pot Photocatalytic Environment Protection Reactions. *ACS Appl Mater Interfaces*. 2017.
32. Aryal S, Hu CM, Zhang L. Synthesis of Ptsome: a platinum-based liposome-like nanostructure. *Chem Commun (Camb)*. 2012; 48: 2630-2632.
33. Gao Z, Ye H, Tang D, Tao J, Habibi S, Minerick A, et al. Platinum-Decorated Gold Nanoparticles with Dual Functionalities for Ultrasensitive Colorimetric in Vitro Diagnostics. *Nano Lett*. 2017; 17: 5572-5579.
34. Wang Q, Li J, An S, Chen Y, Jiang C, Wang X. Magnetic resonance-guided regional gene delivery strategy using a tumor stroma-permeable nanocarrier for pancreatic cancer. *Int J Nanomedicine*. 2015; 10: 4479-4490.
35. Li J, Huang S, Shao K, Liu Y, An S, Kuang Y, et al. A choline derivate-modified nanoprobe for glioma diagnosis using MRI. *Sci Rep*. 2013; 3: 1623.
36. Liu L, Bi Y, Zhou M, Chen X, He X, Zhang Y, et al. Biomimetic Human Serum Albumin Nanoparticle for Efficiently Targeting Therapy to Metastatic Breast Cancers. *ACS Appl Mater Interfaces*. 2017; 9: 7424-7435.
37. Rabinovich GA, Gabrilovich D, Sotomayor EM. Immunosuppressive strategies that are mediated by tumor cells. *Annu Rev Immunol*. 2007; 25: 267-296.
38. He R, Tan L, Browning DD, Wang JM, Ye RD. The synthetic peptide Trp-Lys-Tyr-Met-Val-D-Met is a potent chemotactic agonist for mouse formyl peptide receptor. *J Immunol*. 2000; 165: 4598-4605.
39. Vacchelli E, Ma Y, Baracco EE, Sistigu A, Enot DP, Pietrocola F, et al. Chemotherapy-induced antitumor immunity requires formyl peptide receptor 1. *Science*. 2015; 350: 972-978.
40. Simpson S, Jr., Stewart N, van der Mei I, Otahal P, Charlesworth J, Ponsonby AL, et al. Stimulated PBMC-produced IFN-gamma and TNF-alpha are associated with altered relapse risk in multiple sclerosis: results from a prospective cohort study. *J Neurol Neurosurg Psychiatry*. 2015; 86: 200-207.
41. Abe R, Donnelly SC, Peng T, Bucala R, Metz CN. Peripheral blood fibrocytes: differentiation pathway and migration to wound sites. *J Immunol*. 2001; 166: 7556-7562.